International Journal of Nanomedicine

Dovepress
open access to scientific and medical research

Open Access Full Text Article

ORIGINAL RESEARCH

Hyaluronic acid-modified mesoporous silica-coated superparamagnetic Fe_3O_4 nanoparticles for targeted drug delivery

This article was published in the following Dove Press journal:
International Journal of Nanomedicine

Zhengzou Fang[1]
Xinyuan Li[2]
Zeyan Xu[3]
Fengyi Du[3]
Wendi Wang[1]
Ruihua Shi[4]
Daqing Gao[1]

[1]Department of Pathogenic Microbiology and Immunology, Southeast University School of Medicine, Nanjing 210009, People's Republic of China; [2]Department of Clinical Laboratory, Huai'an Hospital Affiliated to Xuzhou Medical College and Huai'an Second Hospital, Huai'an, Jiangsu, People's Republic of China; [3]Department of Gastroenterology, Jiangsu University, School of Medicine, Zhenjiang 212013, People's Republic of China; [4]Department of Gastroenterology, Affiliated Zhongda Hospital, Southeast University, Nanjing 210009, People's Republic of China

Introduction: The targeted delivery of anti-cancer drugs to tumor tissue has been recognized as a promising strategy to increase their therapeutic efficacy and reduce side effects. Mesoporous silica-coated superparamagnetic Fe3O4 nanoparticles (NH2-MSNs), a kind of nanocarrier, can passively enter tumor tissues to enhance the permeability and retention of drugs. However, NH2-MSNs do not specifically bind to cancer cells. This drawback encouraged us to develop a more efficient nanocarrier for cancer therapy.

Methods: Herein, we describe the development of an effective nanocarrier based on NH2-MSNs, which were modified with hyaluronic acid on their surface (HA-MSNs) and loaded with doxorubicin (DOX). We have successfully fabricated uniform spherical HA-MSNs nanocarriers. The targeting ability of this delivery system was evaluated through specific uptake by cells and IVIS imaging.

Results: DOX-HA-MSNs nanocarriers displayed more dramatic cytotoxic activity against 4T1 breast cancer cells compared to GES-1 gastric mucosa cells. In vivo results revealed that once DOX-HA-MSNs nanocarriers are exposed to an external magnetic field, they could be rapidly attracted to the magnet and effectively cross the cytoplasmic membrane via CD44 receptor-mediated transcytosis. This allows them to access the cancer cell cytoplasm and release DOX based on changes in the physiological environment. Both in vitro and in vivo results demonstrated that the HA-MSNs nanocarriers provided better therapeutic efficacy.

Conclusion: The HA-MSNs nanocarriers represent an effective new paradigm to treat cancers due to active targeting to the tumor cells. Moreover, the specific uptake by the tumor effectively protects normal tissues to reduce off-target side effects. The reported findings support further investigation of HA-MSNs for cancer therapy.

Keywords: target-delivery, HA-MSNs, nanocarrier, receptor-mediated, cancer therapy

Introduction

Cancer is a complex, multifactorial disease threatening human health. Many types of cancers are characterized by high mortality and recurrence rates, which encouraged us to develop advance therapeutic methods.[1] Systemic treatment with chemotherapeutic drugs can somewhat restrain tumor growth, but most systemic agents lack the ability to discriminate between malignant and normal cells, resulting in side effects and non-specific cytotoxicity.[2,3] Nanoparticle-mediated targeted drug delivery systems are considered to be plausible strategies to address this problem. Nanoparticles have been verified to be capable of passive accumulation in tumors through the enhanced permeability and retention (EPR) effect.[4,5] As a result, research on multifunctional nanoparticles as drug delivery system has been increasing, and new delivery systems are emerging as a promising modality for the treatment of cancer.

Correspondence: Daqing Gao
School of Medicine, Southeast University, Ding JiaQiao Street 87, Nanjing, Jiangsu 210009, People's Republic of China
Tel +86 258 327 2506
Email dgao2@seu.edu.cn

submit your manuscript | www.dovepress.com
DovePress
http://doi.org/10.2147/IJN.S213974

In recent years, core-shell architectural magnetic mesoporous silica nanoparticles have received increasing attention due to their excellent water dispersibility, biocompatibility and diverse biomedical applications.[6–9] As a drug delivery system, mesoporous silica nanoparticles have a high surface area, a uniform mesoporous surface, large pore volume, easily modifiable surface, excellent biocompatibility and convenient drug-loading.[10–12] More importantly, silica coating is a favorable method for overcoming the toxicity associated with heavy metallic nanoparticles, because the silica shell possesses biochemical stability and resistance to erosion under extreme conditions.[13,14] However, the application of mesoporous silica nanoparticles has been hampered due to the lack of specific localization of therapeutic agents at the tumor site. This drawback prompted us to develop novel nanoparticles for the theranostics of cancer utilizing the intrinsic properties of magnetic mesoporous silica nanoparticles.

Hyaluronic acid (HA), a natural high molecular weight anionic mucopolysaccharide, exhibits good biodegradation, biocompatibility, non-toxic and non-immunogenic. These advantages have led to hyaluronic acid becoming widely applied in biomedicine.[15,16] CD44 is overexpressed in many kinds of tumor cells (REF). Importantly, CD44 can specifically bind with hyaluronic acid.[17,18] In recent decades, HA-amphiphilic derivatives, HA-drug conjugates, HA-surface modified drugs and HA gene targeting drug systems have been widely researched and applied for tumor targeting.[19,20] It was previously reported that the glutathione (GSH) concentration in cancer cells was much higher than that in plasma and normal tissue. Redox-responsive HA-modified mesoporous silica nanoparticles (MSNs-SS-HA) increased the drug release in the targeted sites, and this was attributed to the high GSH concentration in the cancer tissue.[21,22] We therefore elected to incorporate HA in our new nanoparticle drug targeting system.

In this study, we designed safe and effective tumor-targeted hyaluronic acid-modified mesoporous silica-coated superparamagnetic Fe_3O_4 nanoparticles (HA-MSNs), which can accumulate in tumor tissues to enhance the therapeutic effects of conventional agents against cancer cells. Importantly, these HA-MSNs can serve as a bifunctional nanosystem, which can specifically target tumor cells in the tumor microenvironment and efficiently release antitumor drug in response to pH changes. These newly-designed HA-MSNs represent a novel platform for cancer therapy.

Materials and methods

Materials

Anhydrous ferric chloride ($FeCl_3$), cetyl trimethyl ammonium bromide (CTAB), ammonia, ethanol, tetraethyl orthosilicate (TEOS) and (3-aminopropyl) triethoxysilane (APTES) were purchased from Aladdin (Shanghai, China). Hyaluronic acid (HA), DAPI, the lactate dehydrogenase activity assay kit (LDH) and 3-(4,5-dimethylthiazol-2-yl)-2,5-diphenyltetrazolium bromide (MTT) were obtained from Sigma–Aldrich Chemicals (Madison, USA). N-hydroxysuccinimide (NHS) and 1-ethyl-3-(3-dimethylaminopropyl) carbodiimidehydrochloride (EDC·HCl) were purchased from Aladdin (Shanghai, China). Anhydrous sodium acetate (NaOAc), hydrochloric acid (HCl), ethylene glycol and trisodium citrate (Na_3Cit) were of analytical grade and were purchased from Sinopharm Chemical Reagent Co. Ltd. (Shanghai, China). All chemicals were used without further purification. Distilled and deionized water were used throughout the experiments.

Methods

Synthesis of Fe_3O_4 nanoparticles

$FeCl_3$ (2 mmol) was added to 20 mL DEG solution with continuous stirring for 1 hr at 1000 rpm to form a clear solution. Then, NaCit (0.8 mmol) was added to the above solution and the mixture was heated to 80°C with continuous stirring. NaOAc (6 mmol) was dissolved in the above solution for 30 min to obtain a homogenous solution. This mixture was transferred into a Teflon-lined stainless-steel autoclave, and heated to 200°C for 10 h. After being cooled to room temperature, the black products were collected using a magnet and were washed three times with ethanol. The black products were dried at 60°C for further use.[23]

Surface modification of MSNs

Amine-functionalized mesoporous silica-coated Fe_3O_4 nanoparticles (NH_2-MSNs) were modified based on a previous protocol.[24] In brief, 0.1 g of Fe_3O_4 nanoparticles were added into 50 mL of 0.1 M HCl aqueous solution and ultrasonicated for 15 min. These magnetic nanoparticles were washed with deionized water three times and dispersed in a solution containing 80 mL ethanol, 20 mL deionized water and 1 mL 28% ammonia aqueous solution with continuous stirring at 600 rpm. After 1 hr, 30 µL tetraethyl orthosilicate (TEOS) was added dropwise to obtain silica-modified nanoparticles. After 6 hrs, the

products were separated and washed three times with ethanol.[25]

The products were homogenously dispersed in a mixture of 0.3 g cetyl trimethyl ammonium bromide (CTAB), 70 mL ethanol, 80 mL deionized water and 1.2 mL 28% ammonia aqueous solution for 1 h. Then, 0.3 mL TEOS and 0.5 mL APTES were added to the above mixture and continuously stirred for 12 at 37°C. These magnetic nanoparticles were separated and washed with ethanol and deionized, then were dispersed in 60 mL of 1% NH_4NO_3 solution for 12 h. The products were separation by a magnet, washed with ethanol, and dried at 60°C.[26]

Hyaluronic acid conjugation on NH_2-MSNs (generation of HA-MSNs)

A total of 0.15 g HA, 0.1 g EDC.HCl and 0.6 g NHS was added into 100 mL PBS. One hour later, 0.15 g NH_2-MSNs was added to the above solution with continuous stirring for 24 h at room temperature.[27] The final product was obtained by centrifuging the solution at 5000 rpm for 30 min, washed the precipitate with deionized water three times and dried at 60°C.[28]

The characterization of nanoparticles

The size and shape of the nanoparticles were observed by transmission electronic microscopy (TEM, JEOL-2100). For the TEM study, the nanoparticles were dispersed in deionized water and ultrasonicated for 10 min. The solution was then dropped onto a carbon-coated copper grip, air-dried, and the images were taken.[29] The surface morphology of the nanoparticles was analyzed by scanning electron microscopy (SEM). The accelerating voltage was 10 kV and the observation time was as short as possible.[30] The hyaluronic acid conjugation with NH_2-MSNs was analyzed by UV-Vis spectrophotometry.[31] The modification of Fe_3O_4 nanoparticles at each step was determined by FTIR spectra. Each sample used for the FTIR spectral analysis was prepared in the range 500–4000 cm^{-1}.[32] The surface functional groups and the composition of HA-MSNs were confirmed by XPS analysis using an AI Kα excitation source in an ESCA-2000 Multilab apparatus (VG microtech) with a model Nexus-870 (Thermo Nicolet Corporation, Wisconsin, USA). A N_2 absorption-desorption instrument was used to measure the surface area, pore size and pore distribution of the HA-MSNs (Quantachrome Corporation, Quantachrome Autosorb Automated Gas Sorption System, USA).[33]

Cell culture

Murine 4T1 breast cancer cells, anthropogenic SW480 colon cancer cells, anthropogenic GES-1 gastric mucosa cells and anthropogenic HepG2 hepatoma carcinoma cells were obtained from Jiangsu University (Zhenjiang, China) and were cultivated at 37°C in a 5% CO_2 incubator. The cell medium was RPMI 1640 Medium (1640) (Gibco, Shanghai, China) containing 10% fetal calf serum (FCS) (Gibco, Shanghai, China). All the cell lines were approved by the Institutional Animal Care and Use Committee of Southeast University.

Cell viability and cytotoxicity assay

The influence of HA-MSNs and NH_2-MSNs on cell viability was assessed using the Cell Counting Kit 8 assay (CCk-8, assay). GES-1 cells, 4T1 cells, HepG2 cells and SW480 cells were seeded into 96-well plates at a density of 3×10^4 cells per well and cultured at 37°C in 5% CO_2 incubator for 24 hrs, then the medium was replaced with fresh 1640 media containing 10% FBS and different concentrations of HA-MSNs and NH_2-MSNs (0 μg/mL, 5 μg/mL, 10 μg/mL, 25 μg/mL or 50 μg/mL). After 24 hrs, 10 μL CCK-8 solution was added to each well, then cells were incubated for 3 hrs in dark place. The absorbance was subsequently measured at 405 nm using a Synergy HT Multi-Mode Microplate Reader (Bio Tek, Winooski, VT, USA). Untreated cells were used as a control, and the relative cell viability (mean and SD, n=3) was expressed as the Test Sample/Control Sample.[25] The cytotoxicity of HA-MSNs and NH_2-MSNs was evaluated using an LDH assay kit following the above protocol. The following equation was used to calculate the cytotoxicity: cytotoxicity = (test sample−low control)/(high control−low control). The tests were performed in triplicate for each sample.[28]

Drug loading and release of HA-MSNs

A total of 10 mg of HA-MSNs were dispersed in 10 mL of PBS solution including 5 mg doxorubicin (DOX) and stirred at room temperature for 24 hrs in a dark environment. DOX-loaded HA-MSNs (DOX-HA-MSNs) were collected by centrifugation and washed with PBS. The supernatant DOX solution was collected to evaluate the DOX loading capacity. The DOX loading content was determined by UV-vis at 480 nm. The loading content was calculated using the equation: Loading content = (initial weight of drug−weight of drug in supernatant)/weight of drug-loaded nanoparticles. The DOX-loaded NH_2-MSNs were prepared using a similar method.[34,35]

To investigate the drug release by the nanoparticles, 10 mg of DOX-HA-MSNs were immersed into 10 mL PBS solution at different pH values (pH =5.5 and 7.4). The mixtures were incubated at 37°C with shaking at 200 rpm. As designed time points, 1 mL of solution was withdrawn, and the amount of released drug was determined by UV-vis.[24]

In vitro tumor-targeted drug delivery of HA-MSNs

The internalization and intracellular distribution of DOX-HA-MSNs were observed by fluorescence microscopic imaging. The DOX-HA-MSNs were incubated with GES-1 cells and 4T1 cells. After the cells were treated with 5 mg/mL DOX-HA-MSNs in the culture for 4 h, the culture media were removed, and the cells were washed three times with PBS. The cells were then stained with DAPI for 10 min at room temperature and observed by fluorescence microscopy.[36,37]

Animal welfare

In this study, all animal experiments were executed according to a protocol approved by the Animal Management Rules of the Ministry of Health of the People's Republic of China and approved by the Institutional Animal Care and Use Committee of Southeast University. Female 6- to 8-week-old BALB/c mice were purchased from Yangzhou University (Yangzhou, People's Republic of China) and maintained under specific pathogen-free-conditions. All efforts were made to minimize the animals' suffering and to reduce the number of animals used.

In vivo treatment of subcutaneous xenograft tumors

Subcutaneously xenograft tumors were established by injected 1×10^7 4T1 cells into male mice.[38] When the tumor volume reached approximately 50 mm^3, tumor-bearing mice were randomized into 6 groups (n=6/group) and treated with PBS, free DOX (1 mg/kg), DOX-NH_2-MSNs (DOX =1 mg/kg, particle concentration =4 mg/kg), DOX-HA-MSNs (DOX =1 mg/kg, particle concentration =4 mg/kg), HA-MS (particle concentration =4 mg/kg) or HA-MSNs (particle concentration =4 mg/kg) by tail vein injection every 3 days.[36,37] After injection, a small magnet was placed on the tumor site of the mice for 0.5 h. The injections were repeated seven times over a 22-day treatment period. The body weights of the mice and tumor growth were monitored every day. The tumor volume was measured according to the following formula: Tumor volume = $width^2\times length\times0.5$. After 22 days, all mice were sacrificed, and the tumors were excised and weighed.

Histological analysis

After the 22-day treatment, the animals were sacrificed and all major organs, including the heart, liver, spleen, lung and kidney, were removed a histological analysis. After removal, the tissues were fixed with 4% formalin and then embedded in paraffin. Tissue sections were made and stained with hematoxylin and eosin (H&E). The evaluations of the tissue slices were conducted by an experienced pathologist.[39,40]

In vivo imaging and biodistribution analysis

Tumor-bearing mice were injected through a tail vein with 200 μl of PBS, DOX, DOX-HA-MS, DOX-NH_2-MSNs, DOX-HA-MSNs or HA-MSNs. IVIS, an in vivo imaging system, was used to generate ex vivo images of mice. Light with a wavelength at 500 nm was used as the excitation source. After 24 hrs injection, the mice were sacrificed and the heart, liver, spleen, lung, kidney and tumor tissue were collected from each mouse. The fluorescence intensity in all organs was analyzed by the IVIS Spectrum in vivo imaging system.[41]

Statistical analysis

Data were expressed as the means ± SD. The statistical significance of the data were determined by Student's *t*-tests. Statistical significance was inferred at a value of $P<0.05$.

Results and discussion

HA-MSNs with superparamagnetic properties are a versatile carrier for targeted therapeutics. The detailed procedure for the preparation of HA-MSNs is illustrated in Scheme 1. First, water-dispersible Fe_3O_4 cores were synthesized through a solvothermal route using ethylene glycol as a reducing agent. Next, a modified sol-gel process was developed to decorate the surface of Fe_3O_4 with TEOS and produce silica-coated Fe_3O_4 nanoparticles. Further, APTES was used as a silane precursor to introduce amine functionalities on the nanoparticles, and CTAB was used as the pore-forming agent. The CTAB was subsequently removed from amine-functionalized mesoporous silica-coated magnetic Fe_3O_4 nanoparticles (NH_2-MSNs). Thereafter, hyaluronic acid (a cancer cell-targeting ligand) was conjugated to the amine group on the surface of NH_2-MSNs via the formation of amide bonds (HA-MSNs).[42,43]

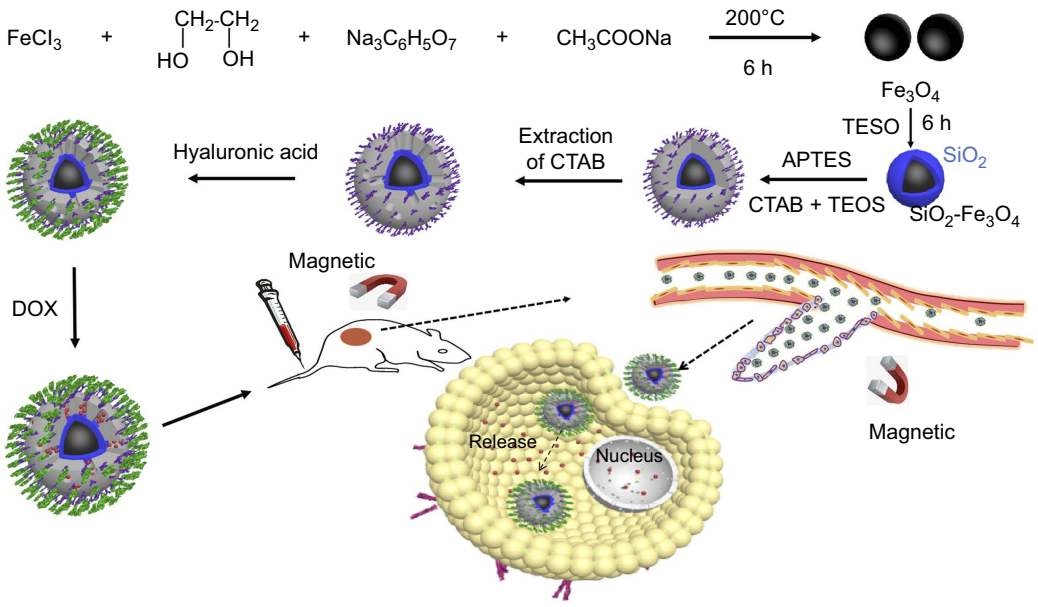

Scheme 1 Schematic illustration of the fabrication of the HA-MSNs and their application for pH-responsive drug release after specific binding with cancer cells, as well as targeted cancer therapy in vivo.

Doxorubicin (DOX), used as a model anticancer drug, was loaded into the porous structure of the HA-MSNs shell. After intravenous injection, the HA-MSNs were expected to accumulate in cancer tissues as a combined function of the magnetic targeting-enhanced EPR effect and HA-mediated active targeting. After being taken up by cancer cells, the loaded DOX would be released from the mesoporous silica shell to induce cancer cell death.

The surface chemistry and conjugation of different functional moieties were investigated by Fourier transform infrared (FTIR) spectroscopy. The FTIR spectra of Fe_3O_4, amine-functionalized mesoporous silica-coated Fe_3O_4 nanoparticles (NH_2-MSNs), and hyaluronic acid-modified mesoporous silica-coated superparamagnetic Fe_3O_4 nanoparticles (HA-MSNs) are shown in Figure 1A. In all spectra, the peaks at 3470 cm^{-1} and 610 cm^{-1} were attributed to vibrational modes of O-H stretching.[25] In the spectra of NH_2-MSNs and HA-MSNs, peaks at 1358 cm^{-1} and 1057 cm^{-1} correspond to C-H binding and Si-O-Si stretching vibrations, respectively.

Two peaks were seen at 2936 cm^{-1} and 2856 cm^{-1} at NH_2-MSNs may be attributed to the presence of asymmetric CH_2 stretching and symmetric CH_2 stretching on NH_2-MSNs. Additionally, one peak at 740 cm^{-1} may be ascribed to the presence of APTES on the nanoparticles. After modification by hyaluronic acid, one new peak

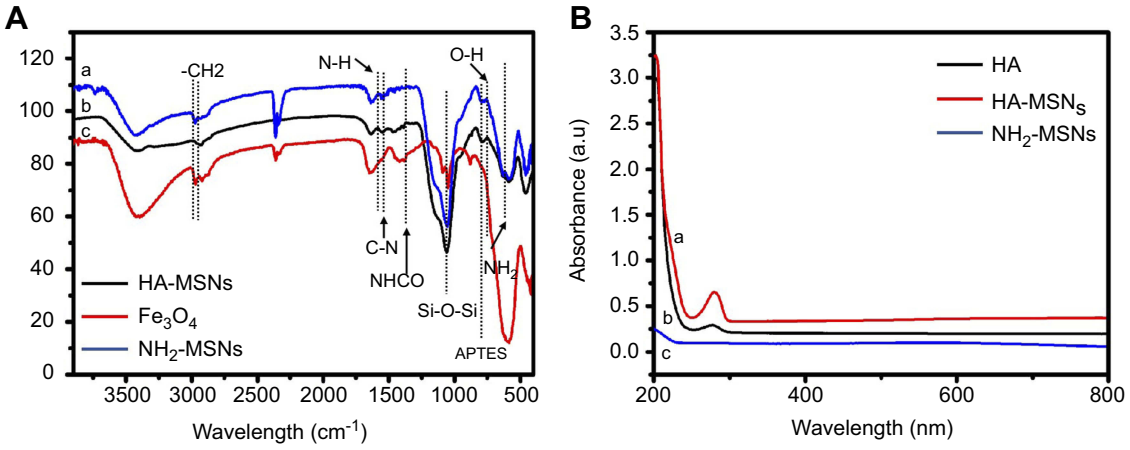

Figure 1 (**A**) FTIR spectra of (**A**) HA-MSNs, (**B**) NH_2-MSNs and (**C**) Fe_3O_4. (**B**) UV-Vis absorbance of (**A**) HA-MSNS, (**B**) HA, (**C**) NH_2-MSNs.

appeared at 1230 cm^{-1}, which corresponds to the formation of an amide bond. As shown in Figure 1B, conjugation of hyaluronic acid on the NH_2-MSNs was confirmed by UV-Vis spectroscopy. Hyaluronic acid exhibited one band at 285 nm owing to the π-π* transitions corresponding to the HA molecule. No peaks were detected in NH_2-MSNs, whereas one peak was observed in HA-MSNs corresponding to free HA, suggesting that HA had attached to the NH_2-MSNs.[21]

XPS is a useful technique to understand the elemental composition and functional groups of a compound. As shown in Figure 2A, the as-produced HA-MSNs had five peaks at 711.36, 532.27, 400.5, 285.86 and 102.93 eV, which indicated that the HA-MSNs were composed of Si, C, N, O and Fe, with atomic percentages of 18.49, 28.16, 5.16, 46.91 and 1.28%, respectively. The spectra for Fe 2p in the HA-MSN nanoparticles were obtained at 710.516 eV and 724.081 eV for Fe $2p_{3/2}$ and Fe $2p_{1/2}$, respectively (Figure 2B).[24] As shown in Figure 2C, the spectrum for Si 2p had a Si peak at 102.67 eV corresponding to Si-O. Since the hyaluronic acid was attached to the NH_2-MSNs via amide bonds, the peak for the amide bond confirmed the conjugation of hyaluronic acid to NH_2-MSNs. For the N 1s element (Figure 2D), the spectrum could be deconvoluted into two peaks corresponding to binding energy values of 399.5 eV and 401.5 eV for the $-NH_2$ and -NHCO groups (respectively), demonstrating that amine and amide groups were present in the nanoparticles. Figure 2E showed two peaks for the deconvoluted spectra of the O 1s element, one at 532.09 eV and the other at 532.8 eV, for C-O and NH-CO, respectively. As shown in Figure 2F, the C 1s peak can be deconvoluted into three peaks corresponding to the binding energy values of 284.45 eV, 285.54 eV and 286.4 eV for C-C/C-H, C-O and C-O-C, respectively. These result also confirmed that the hyaluronic acid was successfully conjugated to the NH_2-MSN nanoparticles.[35]

The structure of HA-MSNs was observed by a transmission electron microscope (TEM) and a SEM. As indicated in Figure 3A, the dark core of Fe_3O_4 nanoparticles was almost spherical, with a uniform size ranging from 90 to110 nm. One typical Fe_3O_4 nanoparticle and the distribution of Fe_3O_4 nanoparticles diameter were shown in the inset of Figure 3A. After being coated with mesoporous silica, the average size of HA-MSNs with the inner black magnetic core was found to be approximately 160 nm and the mainly particles size distribution were shown in the inset of Figure 3B. SEM images of HA-MSNs with nanoscaled structures are shown in Figure 3C, demonstrating that the morphology of the prepared nanoparticles was almost spherical.[25]

The porous structure of the HA-MSNs was confirmed by a nitrogen absorption-desorption isotherms plot (Figure 3D). As shown in Figure 3E, the Brunauer-Emmett-Teller (BET)

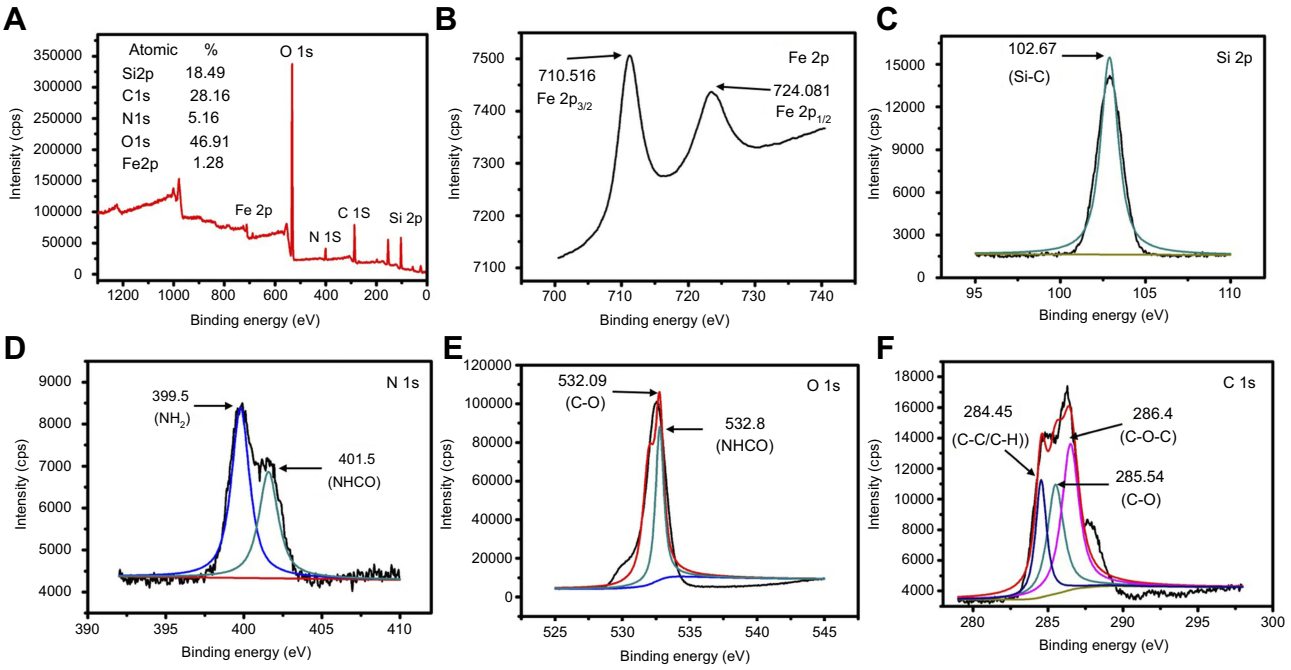

Figure 2 XPS spectra of HA-MSNs. (**A**) Survey spectrum. (**B**) Fe 2p spectrum. (**C**) Si 2p spectrum. (**D**) N 1s spectrum. (**E**) O 1s spectrum. (**F**) C 1s spectrum.

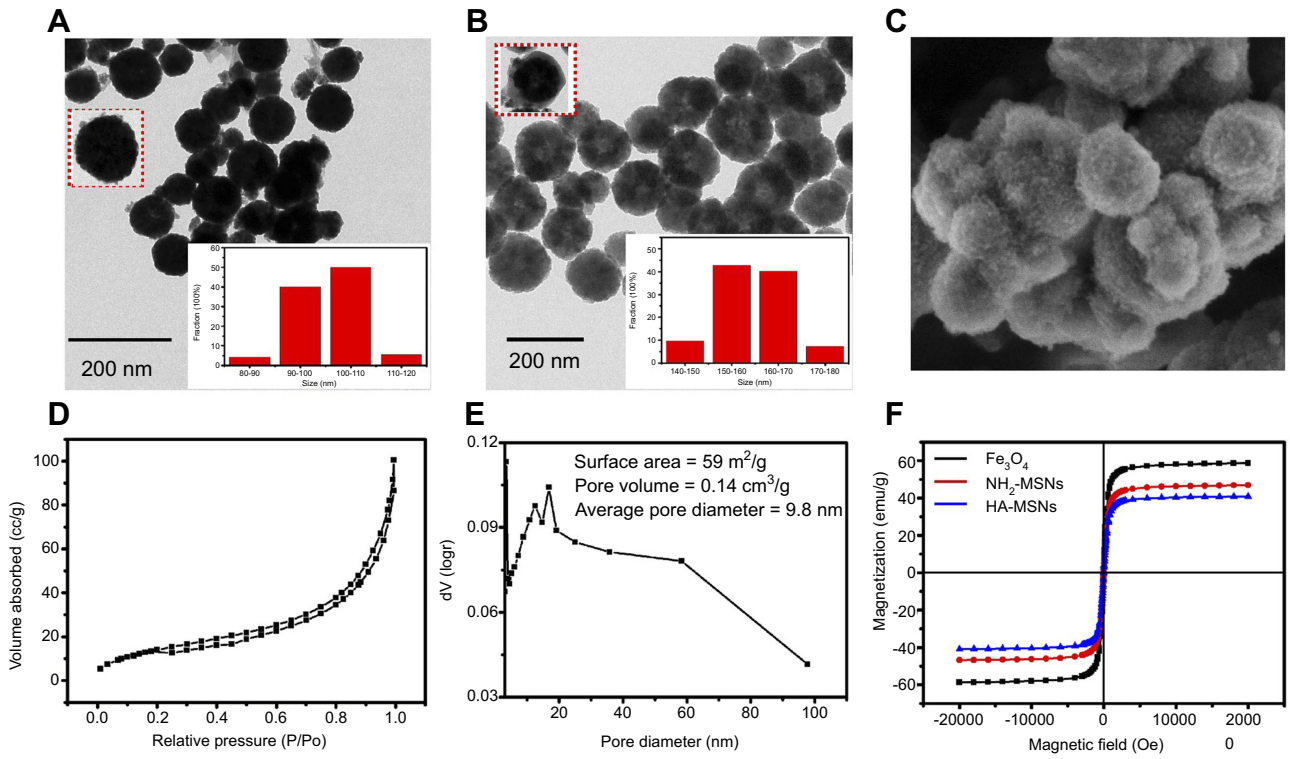

Figure 3 TEM images of (**A**) Fe_3O_4 nanoparticles and (**B**) HA-MSNs nanoparticles. (**C**) A representative SEM image of HA-MSNs. (**D**) The nitrogen adsorption-desorption isotherm pattern. (**E**) The BJH pore distribution of HA-MSNs. (**F**) The VSM curves of Fe_3O_4 nanoparticles, NH_2-MSNs and HA-MSNs.

surface area for HA-MSNs was 59 m^2/g (average) and the average pore volume of HA-MSNs was 0.14 cm^3/g. The BJH pore distributions of HA-MSNs showed an unequal pore size distribution in the range 4–95 nm, with most being around 11 –15 nm, making the average pore diameter 9.8 nm. As Figure 3F showed, the magnetic response of Fe_3O_4, NH_2-MSNs and HA-MSN nanoparticles were analyzed by VSM. The saturated magnetization value for Fe_3O_4 nanoparticles was 59 emu/g which was much higher compared to HA-MSN nanoparticles (41 emu g^{-1}). After NH_2-MSNs nanoparticles was modified with hyaluronic acid, the magnetic response of HA-MSN nanoparticles was slightly reduced 39 emu g^{-1}, and once exposed to an external magnetic field which could be rapidly attracted by a magnet.[26]

The CCK8 assay was used to evaluate the cytotoxicity of the HA-MSNs and NH_2-MSNs in GES-1 cells, 4T1 cells, HepG2 cells and SW480 cells. As shown in Figure 4A, no obvious toxicity was revealed with an increase in the NH_2-MSNs concentration, and the cell viability remained approximately 95% after 24 hrs of incubation with NH_2-MSNs at a concentration of 50 μg/mL. As shown in Figure 4B, the viability of GES-1 cells was largely unchanged. The other groups of cells were approximately 90% viable after 24 hrs of incubation with HA-MSNs at a concentration of 50 μg/mL. These results were confirmed by measuring the cytotoxicity of HA-MSNs and NH_2-MSNs using an LDH assay. The NH_2-MSNs and HA-MSNs exhibited an almost identical influence on cell viability (Figure 4C and D).[28] All of the above results indicate that negligible cytotoxicity was observed in both tumor cells and normal cells, confirming that the HA-MSNs are non-toxic when the concentration is 50 μg/mL or less.

Although doxorubicin (DOX) exerts potent anti-cancer effects, its non-specific side-effects limit its application in the clinic.[44] In this study, DOX was loaded into HA-MSNs to permit tumor-specific targeting. The DOX loading efficiency on HA-MSNs was about 65%, as determined by UV-vis spectrophotometry. Doxorubicin (DOX) can auto-emit red fluorescence (REF). As shown in Figure 5A, the fluorescence of DOX was quenched when it was absorbed onto the pores of HA-MSNs. Figure 5B reveals that DOX was released from the DOX-HA-MSNs in phosphate buffers with different pH values (5.5 and 7.4). However, the DOX-HA-MSNs release DOX more favorably under the acidic condition (pH 5.5). Less than 20% of the DOX was released when the DOX-HA-MSNs were incubated at pH 7.4 for 80 h, while as much as 60% of the DOX was released

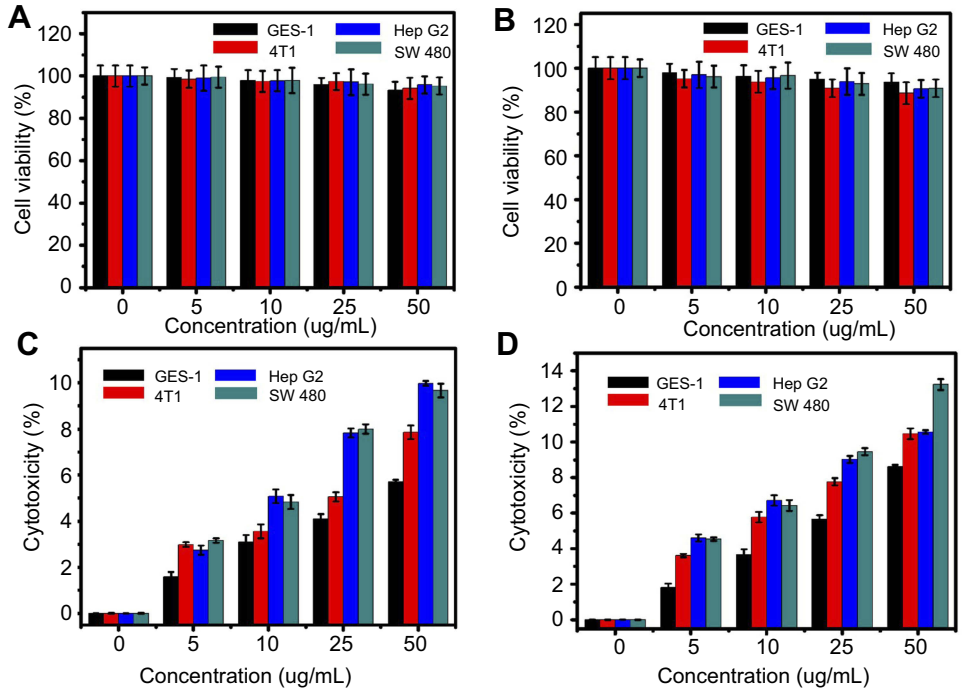

Figure 4 The effects of (**A**) NH_2-MSNs and (**B**) HA-MSN_S at concentrations from 0–50 μg/mL on the viability of GES-1, 4T1, Hep G2 and SW480 cells, as determined by the CCK8 assay. These findings were confirmed by LDH assays of (**C**) NH_2-MSNs and (**D**) HA- MSN_S cultured under the same conditions.

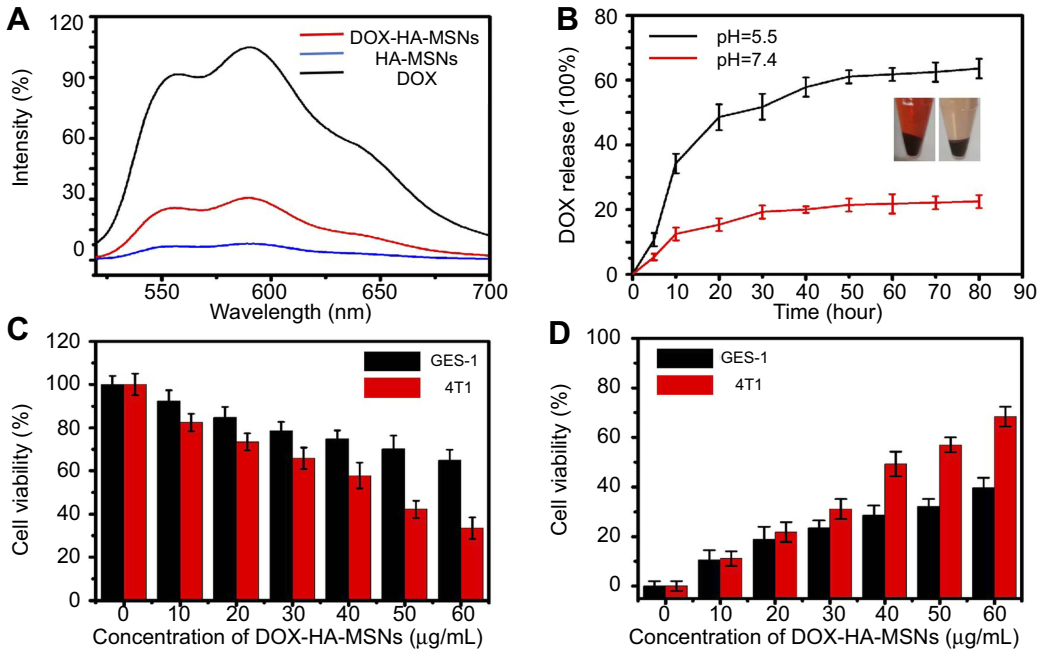

Figure 5 The DOX loading of HA-MSN_S led to the pH-sensitive release of DOX to kill GES-1 and 4T1 cells. (**A**) Fluorescence spectra of free DOX, HA-MSN_S and DOX-HA-MSN_S dispersed in PBS. (**B**) In vitro profiles of DOX-HA-MSN_S under different pH conditions. MTT (**C**) and LDH (**D**) assays of GES-1 and 4T1 cells treated with different concentrations of DOX-HA-MSN_S.

within 80 h at pH 5.5. It is believed that when DOX-HA-MSNs were immersed in a buffer at pH =5.5, the DOX molecules were protonated and readily released into the aqueous medium. Since the tumor environment and other areas of inflammation tend to be more acidic than the normal physiological environment, it is expected that

these areas of higher acidity would permit greater DOX release.[36] The cell viability results from MTT and LDH assays indicated that the DOX-HA-MSNs exhibited higher cytotoxicity against 4T1 cells than GES-1 cells, particularly at the higher concentrations (Figure 5C and D). The pH-responsive release of DOX can be utilized to achieve efficient intracellular delivery. Therefore, we believe that DOX can be released from HA-MSNs based on changes in the physiological environment, including those that occur during conventional anti-cancer therapy.

Confocal laser scanning microscopy was used to visualize the internalization and intracellular distribution of DOX-HA-MSNs by 4T1 cells and GES-1 cells following incubation for 4 h.[45] Compared with 4T1 cells, the red fluorescence intensity was lower in both the nuclei and cytoplasm of GES-1 cells after incubation with DOX-HA-MSNs for 4 h, indicating that there was higher cellular uptake of HA-MSNs by 4T1 cells than by GES-1 cells (Figure 6). This is because CD44 is a cell surface receptor for hyaluronic acid and is overexpressed on the surface of 4T1 cells, resulting in greater DOX internalization by 4T1 cells.[46] These results indicated that DOX-HA-MSNs exhibits enhanced endocytosis and DOX release, thus improving the therapeutic efficacy (as shown in Figure 5C and D).

The excellent anticancer and stimulus-responsive performance of DOX-HA-MSNs in vitro compelled us to examine its in vivo activity. We utilized a 4T1 xenograft tumor model to evaluate the anti-tumor effects of DOX-HA-MSNs in the presence and absence of the HA modification. Mice bearing 4T1 xenograft tumors were randomly divided into six treatment groups (n=6/group), which were administered PBS, DOX, NH_2-MSNs, HA-MSNs, DOX-NH_2-MSNs and DOX-HA-MSNs. As shown in Figure 7, the tumor growth was completely inhibited in the DOX group, with these mice having the lowest tumor volume and tumor weight. However, the body weight in these mice decreased significantly with adynamia, dehydration and fading of the eye color. This indicates that while DOX had excellent anti-tumor effects, it led to severe side effects. Compared to the DOX-NH_2-MSNs group, the DOX-HA-MSNs group exhibited a significantly higher rate of tumor inhibition, indicating that the hyaluronic acid modification of the nanoparticles enhanced the anti-tumor effects. Moreover, the body weights of the mice in the DOX-NH_2-MSNs and DOX-HA-MSNs groups did not differ significantly from that in the control group, and the general status of the mice remained unchanged. These results indicate that DOX-HA-MSNs not only inhibited tumor growth, but also reduced the side effects of DOX. In addition, the HA-MSNs group showed no difference in the tumor volume, tumor weight or mouse body weight compared with the control group. This is because passive targeting will enhance the EPR effect of magnetic theranostic agents specifically in the targeted tumor in vivo.[47] The DOX-HA-MSNs can specifically bind with cancer cells via CD44-mediated endocytosis, allowing for more specific and efficient treatment of cancer.

As shown in Figure 8, the tumor targeting was evaluated by tracking the DOX fluorescent signal, which can be

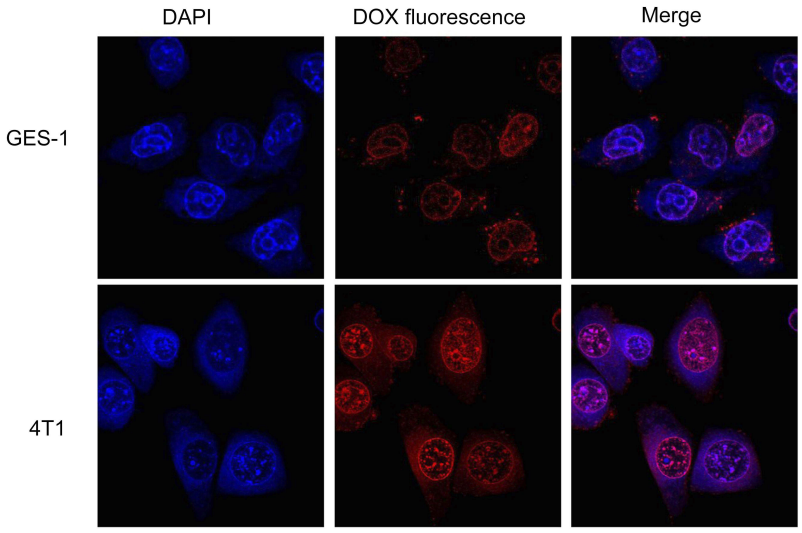

Figure 6 CLSM images of GES-1 and 4T1 cells incubated with DOX-HA-MSNs for 4 h (DOX equivalent dose: 5 μg/mL). Images from left to right show cell nuclei stained by DAPI (blue), DOX fluorescence in cells (red) and the merged overlap of the two images.

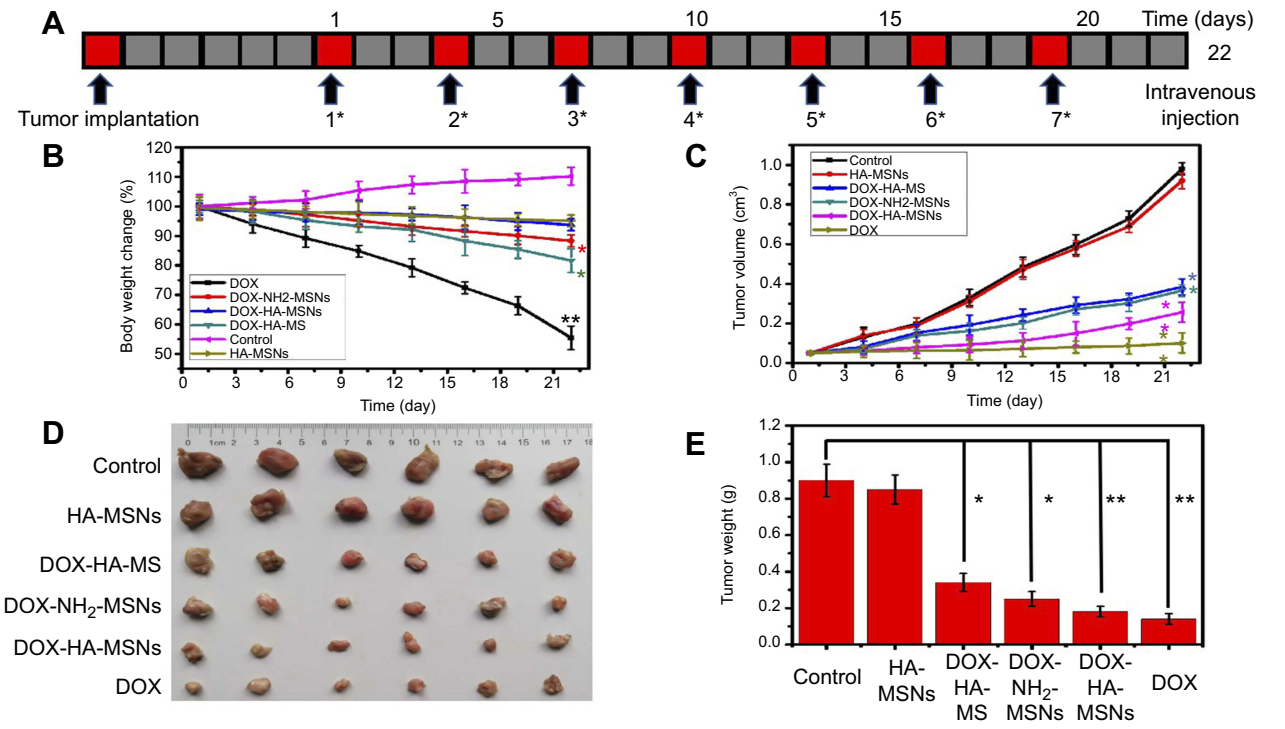

Figure 7 (**A**) 4T1 tumor-bearing mice were administered PBS, DOX, NH_2-MSNs, HA-MSNs, DOX-NH_2-MSNs or DOX-HA-MSNs every 3 days for 22 days via intravenous injection. (**B**) The body weights of PBS-treated mice compared with mice treated with NH_2-MSNs, HA-MSNs, DOX-NH_2-MSNs, and DOX-HA-MSNs and free DOX over the 22 days, (**C**) the tumor volumes in the six groups, (**D**) photographs of the tumors on day 22 and (**D**) the tumor weights on day 22. Data are the mean values ± SD, *p<0.05 and **p<0.01versus the control group.

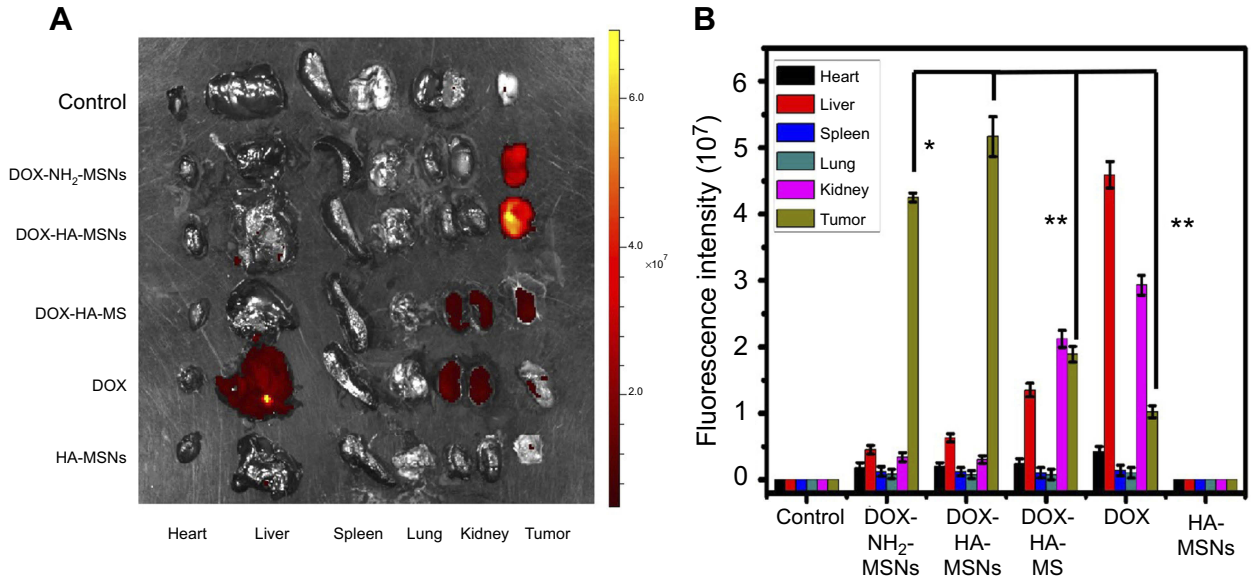

Figure 8 Ex vivo fluorescence imaging of mouse xenograft tumors on day 22 after treatment. (**A**) Ex vivo fluorescence images and (**B**) the quantitative fluorescence analysis of DOX-NH_2-MSNs, DOX-HA-MSNs, NH_2-MSNs, DOX and HA-MSNs in the heart, liver, spleen, lungs, kidneys and tumor of the 4T1 tumor-bearing mice.

used to gauge the quantity and distribution of DOX-HA-MSNs in tumor and other tissues.[41] At 24 h after injection, the fluorescent signal of the DOX-HA-MSNs group was much higher than that of the other groups in tumor tissue (but not other tissues), which confirmed the efficient tumor-targeting and tumor accumulation of the DOX-HA-MSNs. Compared with the DOX-HA-MSNs group, the fluorescent signal of DOX-NH_2-MSNs group was

slightly decreased, which may be attributed to hyaluronic acid modified nanoparticle can enhance tumor cellular uptake. More importantly, the magnetic field enhanced the retention of the DOX-HA-MSNs in the tumor site more than the DOX-HA-MSNs group treated without the magnetic field, indicating the efficiency of the magnetic targeting. However, in DOX group, only a little fluorescent signal was detected in tumor tissue, while the majority of fluorescence was detected in the liver and kidneys. The mice treated with hyaluronic acid-modified nanoparticles and an external magnetic field had enhanced retention of DOX-HA-MSNs in the tumor site. These results demonstrated that HA-MSNs represent an anticancer drug carrier that can achieve enhanced therapeutic effects and reduced side-effects.

In order to investigate the influences of DOX-HA-MSNs on the major organs, a histological evaluation was carried out to observe the changes in major organs. Tissue slices were prepared from the heart, liver, spleen, lungs and kidneys from the different groups on day 22.[39] As shown in Figure 9, no apparent toxicity was observed for the DOX-HA-MSNs group, and the tissue sections of different organs were found to be normal according to a histological analysis (H&E staining).[40] However, myocardial tissue swelling and lung structural damaged were seen in the DOX group, while the cardiac myocytes lined up in order and the lung structure was normal in the HA-MSNs group. These results demonstrated that HA-MSNs can serve as a safe and effective cancer therapeutic nanocarrier.

Conclusion

In summary, we successfully fabricated pH-sensitive DOX-HA-MSNs functionalized with a target-specific CD44 ligand for drug delivery. TEM images showed that the core-shell structure of the HA-MSNs were in the desired size range for drug delivery applications, suggesting that they should be specifically taken up by cancer cells compared with normal cells. In vitro biological studies revealed that the DOX loading of HA-targeted nanoparticles achieved excellent efficacy for targeting and destroying cancer cells. The DOX-HA-MSNs nanocarriers could efficiently deliver DOX to the tumor tissues, and gradually released DOX in response to the intracellular tumor microenvironment. The DOX-HA-MSNs demonstrated an excellent capacity for targeting and effective anticancer efficacy both in vitro and in vivo. Moreover, the DOX-HA-MSNs nanocarriers exhibited a high tumor-targeting ability, leading to effective tumor growth inhibition without any apparent systemic side effects. Although further studies are needed, the various studies described in this manuscript indicate that the HA-MSNs represent an attractive nanocarrier that should have great potential for the treatment of cancer.

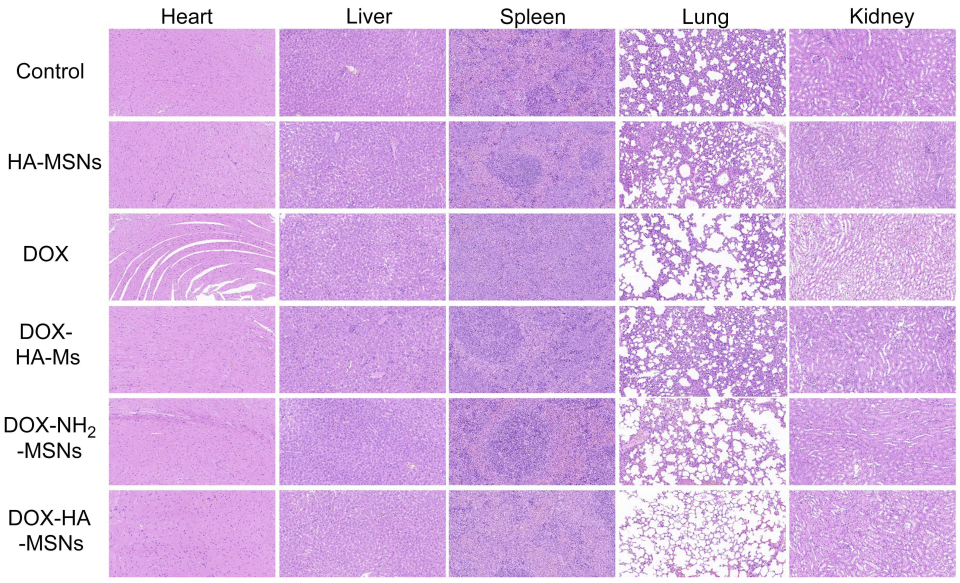

Figure 9 Histological images from the major organs of mice in the different groups of 4T1 tumor-bearing mice on day 22 (n=6). Tissues were collected from the brain, heart, liver, spleen, lung and kidney. Images were taken at ×20 magnification with standard hematoxylin and eosin (HE) staining.

Acknowledgment

This work was supported by the Chinese National Nature and Science Foundation (Grant no. 31570124).

Disclosure

The authors report no conflicts of interest in this work.

References

1. Maluccio M, Covey A. Recent progress in understanding, diagnosing, and treating hepatocellular carcinoma. *CA Cancer J Clin*. 2012;62:394-399.
2. Mary M, Anne C. Recent progress in understanding, diagnosing, and treating hepatocellular carcinoma. *CA Cancer J Clin*. 2012;62:394–399. doi:10.3322/caac.21161
3. Gan L, Zhenjiang L, Chao S. Obesity linking to hepatocellular carcinoma: a global view. *Biochim Biophys Acta Rev Cancer*. 2018;1869:97–102. doi:10.1016/j.bbcan.2017.12.006
4. Maeda H, Wu J, Sawa T, Matsumura Y, Hori K. Tumor vascular permeability and the EPR effect in macromolecular therapeutics: a review. *J Control Release*. 2000;65:271–284.
5. Maeda H, Sawa T, Konno T. Mechanism of tumor-targeted delivery of macromolecular drugs, including the EPR effect in solid tumor and clinical overview of the prototype polymeric drug SMANCS. *J Control Release*. 2001;74:47–61.
6. Porta F, Lamers GE, Morrhayim J, et al. Folic acid-modified mesoporous silica nanoparticles for cellular and nuclear targeted drug delivery. *Adv Healthc Mater*. 2013;2:281–286. doi:10.1002/adhm.201200176
7. Zhang Q, Wang X, Pei-Zhou L, et al. Cancer treatment: biocompatible, uniform, and redispersible mesoporous silica nanoparticles for cancer-targeted drug delivery in vivo. *Adv Funct Mater*. 2014;24:1–12.
8. Shen S, Tang H, Zhang X, et al. Targeting mesoporous silica-encapsulated gold nanorods for chemo-photothermal therapy with near-infrared radiation. *Biomaterials*. 2013;34:3150–3158. doi:10.1016/j.biomaterials.2013.01.051
9. Teng IT, Chang YJ, Wang LS, et al. Phospholipid-functionalized mesoporous silica nanocarriers for selective photodynamic therapy of cancer. *Biomaterials*. 2013;34:7462–7470. doi:10.1016/j.biomaterials.2013.06.001
10. Li Z, Zhang Y, Feng N. Mesoporous silica nanoparticles: synthesis, classification, drug loading, pharmacokinetics, biocompatibility, and application in drug delivery. *Expert Opin Drug Deliv*. 2019;16:219–237. doi:10.1080/17425247.2019.1575806
11. Bau L, Bartova B, Arduini M, Mancin F. Surfactant-free synthesis of mesoporous and hollow silica nanoparticles with an inorganic template. *Chem Commun (Camb)*. 2009;48:7584–7586. doi:10.1039/b917561j
12. Gao Y, Chen Y, XueFeng J, et al. Controlled intracellular release of doxorubicin in multidrug-release cancer cells by tuning the shell-pore sizes of mesoporous silica nanoparticles. *ACS Nano*. 2011;5:9788–9798. doi:10.1021/nn2033105
13. Tarn D, Ashley CE, Xue M, Carnes EC, Zink JI, Brinker CJ. Mesoporous silica nanoparticle nanocarriers: biofunctionality and biocompatibility. *Acc Chem Res*. 2013;46:792–801. doi:10.1021/ar3000986
14. Lee JE, Lee N, Kim H, et al. Uniform mesoporous dye-doped silica nanoparticles decorated with multiple magnetite nanocrystals for simultaneous enhanced magnetic resonance imaging, fluorescence imaging, and drug delivery. *J Am Chem Soc*. 2010;132:552–557. doi:10.1021/ja905793q
15. Yen WC, Lamph WW. A selective retinoid X receptor agonist bexarotene (LGD 1069, Targretin) prevents and overcomes multidrug resistance in advanced prostate cancer. *Prostate*. 2006;66:305–331. doi:10.1002/pros.20455
16. Yadav AK, Mishra P, Jain S, Mishra P, Mishra AK, Agrawal GP. Preparation and characterization of HA-PEG-PCL intelligent core-corona nanoparticles for delivery of doxorubicin. *J Drug Target*. 2008;16:464–478. doi:10.1080/10611860802095494
17. Ghosh SC, Alpay N, Klostergaard J. CD44: a validated target for improved delivery of cancer therapeutics. *Expert Opin Ther Targets*. 2012;16:635–650. doi:10.1517/14728222.2012.687374
18. Cohen K, Emmanuel R, Koisin-Finfer E, Shabat D, Peer D. Modulation of drug resistance in ovarian adenocarcinoma using chemotherapy entrapped in hyaluronan-grafted nanoparticle clusters. *ACS Nano*. 2014;8:2183–2195. doi:10.1021/nn500205b
19. Vangara KK, Liu JL, Palakurthi S. Hyaluronic acid-decorated PLGA-PEG nanoparticles for targeted delivery of SN-38 to ovarian cancer. *Anticancer Res*. 2013;33:2425–2434.
20. Mattheolabakis G, Milane L, Singh A, Amiji MM. Hyaluronic acid targeting of CD44 for cancer therapy: from receptor biology to nanomedicine. *J Drug Target*. 2015;23:605–618. doi:10.3109/1061186X.2015.1052072
21. Zhang J, Sun Y, Tian B, et al. Multifunctional mesoporous silica nanoparticles modified with tumor-shedable hyaluronic acid as carriers for doxorubicin. *Colloids Surf B Biointerfaces*. 2016;144:293–302. doi:10.1016/j.colsurfb.2016.04.015
22. Yin S, Huai J, Chen X, et al. Intracellular delivery and antitumor effects of a redox-responsive polymeric paclitaxel conjugate based on hyaluronic acid. *Acta Biomater*. 2015;26:274–285. doi:10.1016/j.actbio.2015.08.029
23. Ganesh S, Iyer AK, Morrissey DV, Amiji MM. Hyaluronic acid based self-assembling nanosystems for CD44 target mediated siRNA delivery to solid tumor. *Biomaterials*. 2013;34:3489–3502. doi:10.1016/j.biomaterials.2013.01.077
24. Zheng W, Gao F, Hongchen G. Magnetic polymer nanospheres with high and uniform magnetite content. *J Magn Magn Mater*. 2005;288:403–410. doi:10.1016/j.jmmm.2004.09.125
25. Sahoo B, Devi KS, Dutta S, Maita TK, Pramanik P, Dhara D. Biocompatible mesoporous silica-coated superparamagnetic manganese ferrite nanoparticles for targeted drug delivery and MR imaging applications. *J Colloid Interface Sci*. 2014;431:31–41. doi:10.1016/j.jcis.2014.06.003
26. Zhang L, Zhang F, Dong W-F, Song J-F, Huo Q-S, Sun H-B. Magnetic-mesoporous Janus nanoparticles. *Chem Communctions*. 2011;47:1225–1227. doi:10.1039/C0CC03946B
27. Chang B, Guo J, Liu C, Qian J, Yang W. Surface functionalization of magnetic mesoporous silica nanoparticles for controlled drug release. *J Mater Chem*. 2010;20:9941–9947. doi:10.1039/c0jm01237h
28. Lin JT, Du JK, Yang YQ, et al. pH and redox dual stimulate-responsive nanocarriers based on hyaluronic acid coated mesoporous silica for targeted drug delivery. *Mater Sci Eng C Mater Biol Appl*. 2017;81:478–484. doi:10.1016/j.msec.2017.08.036
29. Kim K, Kim K, Ryu JH, Lee H. Chitosan-catechol: a polymer with long-lasting mucoadhesive properties. *Biomaterials*. 2015;52:161–170. doi:10.1016/j.biomaterials.2015.02.010
30. Wang F, Wang G, Sun W, Wang T, Chen X. Metallophthalocyanine functionalized magnetic mesoporous silica nanoparticles and its application in ultrasound-assisted oxidation of benzothiophene. *Microporous Mesoporous Mater*. 2015;217:203–209. doi:10.1016/j.micromeso.2015.06.038
31. Zhang M, Fang Z, Zhang X, et al. Hyaluronic acid functionalized nitrogen-doped carbon quantum dots for targeted specific bioimaging. *RSC Adv*. 2016;6:104979–104984. doi:10.1039/C6RA22210B
32. Zhang M, Zhao X, Fang Z, et al. Fabrication of HA/PEI-functionalized carbon dots for tumor targeting, intracellular imaging and gene delivery. *RSC Adv*. 2017;7:3369–3375. doi:10.1039/C6RA26048A
33. Roik NV, Belyakova LA. Interaction of supramolecular centers of silica surface with aromatic amino acid. *J Colloid Interface Sci*. 2011;362:172–179. doi:10.1016/j.jcis.2011.05.085

34. Shao D, Wang Z, Dong WF, et al. Facile synthesis of core-shell magnetic mesoporous silica nanoparticles for pH-sensitive anticancer drug delivery. *Chem Biol Drug Des*. 2015;86:1548–1553. doi:10.1111/cbdd.12622
35. Chen WH, Lei Q, Luo GF, et al. Rational design of multifunctional gold nanoparticles via host-gust interaction for cancer-targeted therapy. *ACS Appl Mater Interfaces*. 2015;7:17171–17180. doi:10.1021/acsami.5b04031
36. Ganta S, Devalapally H, Shahiwala A, Amiji M. A review of stimuli-responsive nanocarriers for drug and gene delivery. *J Control Release*. 2008;126:187–204. doi:10.1016/j.jconrel.2007.12.017
37. Choucair A, Soo PL, Eisenberg A. Active loading and tunable release of doxorubicin from block copolymer vesicles. *Langmuir*. 2005;21:9308–9313. doi:10.1021/la050710o
38. Shao D, Li J, Zheng X, et al. Janus "nano-bullets" for magnetic targeting liver cancer chemotherapy. *Biomaterials*. 2016;100:118–133. doi:10.1016/j.biomaterials.2016.05.030
39. Meng H, Mai WX, Zhang H, et al. Codelivery of an optimal drug/siRNA combination using mesoporous silica nanoparticles to overcome drug resistance in breast cancer in vitro and in vivo. *ACS Nano*. 2013;7:994–1005. doi:10.1021/nn3044066
40. Chen WH, Luo GF, Lei Q, et al. Rational design of multifunction magnetic mesoporous silica nanoparticle for tumor-targeted magnetic resonance imaging and precise therapy. *Biomaterials*. 2016;76:87–101. doi:10.1016/j.biomaterials.2015.10.053
41. Yan J, He W, Yan S, et al. Self-assembled peptide-lanthanide nanoclusters for safe tumor therapy: overcoming and utilizing biological barriers to peptide drug delivery. *ACS Nano*. 2018;12:2017–2026. doi:10.1021/acsnano.8b00081
42. Wang Y, Li B, Zhang L, Li P, Wang L, Zhang J. Multifunctional magnetic mesoporous silica nanocomposites with improved sensing performance and effective removal ability toward Hg(II). *Langmuir*. 2012;28:1657–1662. doi:10.1021/la204494v
43. Zhang XL, Niu HY, Li WH, Shi YL, Cai YQ. A core-shell magnetic mesoporous silica sorbent for organic targets with high extraction performance and anti-interference ability. *Chem Commun (Camb)*. 2011;47:4454–4456. doi:10.1039/c1cc10300h
44. Shao D, Li J, Pan Y. et al. Noninvasive theranostic imaging of HSV-TK/GCV suicide gene therapy in liver cancer by folate-targeted quantum dot-based liposomes. *Biomater Sci*;2015. 833–841. doi:10.1039/C5BM00077G
45. Urakawa H, Tsukushi S, Sugiura H, et al. Neoadjuvant and adjuvant chemotherapy with doxorubicin and ifosfamide for bone sarcomas in adult and older patients. *Oncol Lett*. 2014;8:2485–2488. doi:10.3892/ol.2014.2567
46. Pang X, Lu Z, Du H, Yang X, Zhai G. Hyaluronic acid-quercetin conjugate micelles: synthesis, characterization, in vitro and in vivo evaluation. *Colloids Surf B Biointerfaces*. 2014;123:778–786. doi:10.1016/j.colsurfb.2014.10.025
47. Wang C, Sun X, Chen L, et al. Multifunctional theranostic red blood cells for magnetic-field-enhanced in vivo combination therapy of cancer. *Adv Mater*. 2014;26:4794–4802. doi:10.1002/adma.201400158